Bioorganic & Medicinal Chemistry 22 (2014) 721–727

Contents lists available at ScienceDirect

Bioorganic & Medicinal Chemistry

journal homepage: www.elsevier.com/locate/bmc

Near-infrared-fluorescence imaging of lymph nodes by using liposomally formulated indocyanine green derivatives

Taro Toyota [a,b,c], Hiromichi Fujito [d], Akiko Suganami [b], Tomoki Ouchi [e], Aki Ooishi [e], Akira Aoki [f], Kazutaka Onoue [f], Yutaka Muraki [f], Tomoyuki Madono [f], Masanori Fujinami [a], Yutaka Tamura [b], Hideki Hayashi [g,h,*]

[a] Department of Applied Chemistry and Biotechnology, Graduate School of Engineering, Chiba University, 1-33 Yayoi-cho, Inage-ku, Chiba 263-8522, Japan
[b] Department of Bioinformatics, Graduate School of Medicine, Chiba University, 1-8-1 Inohana, Chuo-ku, Chiba 260-8670, Japan
[c] Department of Basic Science, Graduate School of Arts and Sciences, The University of Tokyo, 3-8-1 Komaba, Meguro, Tokyo 153-8902, Japan
[d] Department of Medical System Engineering, Faculty of Engineering, Chiba University, 1-33 Yayoi-cho, Inage-ku, Chiba 263-8522, Japan
[e] Division of Nanoscience, Graduate School of Advanced Integration Science, Chiba University, 1-33 Yayoi-cho, Inage-ku, Chiba 263-8522, Japan
[f] Yamada Chemical Co. Ltd, 1-1 Kamichoshi-cho, Kamitoba, Minami-ku, Kyoto 601-8105, Japan
[g] Center for Frontier Medical Engineering, Chiba University, 1-33 Yayoi-cho, Inage-ku, Chiba 263-8522, Japan
[h] Department of Frontier Surgery, Graduate School of Medicine, Chiba University, 1-8-1 Inohana, Chuo-ku, Chiba 260-8670, Japan

ARTICLE INFO

Article history:
Received 7 October 2013
Revised 5 December 2013
Accepted 7 December 2013
Available online 20 December 2013

Keywords:
Liposome
Indocyanine green (ICG)
Near-infrared (NIR)-fluorescence probe
Phospholipid
Lymph node

ABSTRACT

Liposomally formulated indocyanine green (LP-ICG) has drawn much attention as a highly sensitive near-infrared (NIR)-fluorescence probe for tumors or lymph nodes in vivo. We synthesized ICG derivatives tagged with alkyl chains (ICG-Cn), and we examined NIR-fluorescence imaging for lymph nodes in the lower extremities of mice by using liposomally formulated ICG-Cn (LP-ICG-Cn) as well as conventional liposomally formulated ICG (LP-ICG) and ICG. Analysis with a noninvasive preclinical NIR-fluorescence imaging system revealed that LP-ICG-Cn accumulates in only the popliteal lymph node 1 h after injection into the footpad, whereas LP-ICG and ICG accumulate in the popliteal lymph node and other organs like the liver. This result indicates that LP-ICG-Cn is a useful NIR-fluorescence probe for noninvasive in vivo bioimaging, especially for the sentinel lymph node.

1. Introduction

In the biological and medical sciences, noninvasive imaging technologies such as radioactive isotope imaging,[1–4] ultrasonic echo imaging,[5–7] and nuclear magnetic resonance imaging[8–10] are used. Among these, near-infrared (NIR) fluorescence imaging has drawn much attention because of low tissue autofluorescence and deep penetration of light into tissues at wavelengths between 650 and 900 nm.[11–18]

Both NIR-fluorescent dyes[19–28] and colloidal particles[29–40] are commonly used in biomedical analyses, and NIR-fluorescent carbocyanine dyes are of great interest because of their ease of synthesis, biocompatibility, tunable spectral properties, and exceptionally high molar absorptivity in the NIR region; therefore, they have been extensively used in cellular and animal imaging applications.[41–59] Indocyanine green (ICG) is one of such NIR-fluorescent dyes, and it has recently garnered much attention in detecting sentinel lymph nodes (SLNs)[60–62] owing to its abovementioned characteristics, but more importantly, because it was approved by the Food and Drug Administration in the United States.[63] SLNs are, hypothetically, the first nodes to receive drainage from primary tumors, and detection of these during operation could prevent morbidity of surgery, improve lymph node staging, and thus contribute to survival and quality of life after surgery. Thus far, SLN mapping procedures with ICG have been tested in various types of malignancies and found to be equally useful and less cumbersome than conventional techniques using radioactive colloids or dyes.[60–62,64–67] However, one of the issues to be considered while using this technique is the rapid diffusion characteristic of this dye. Wide blurring of the dye around injection sites and rapid migration of the dye beyond the SLN have been reported, and these could hamper the accuracy and simplicity of detecting SLNs with this technique.

Liposomes, which are closed bilayer membranes composed of phospholipids, have traditionally been of interest to medical researchers for use as drug carriers and recently have been used as colloidal probes for bioimaging because their size allows for the targeting of a specific region of tumor.[68–76] As a result, liposomally formulated ICG (LP-ICG) has been recently considered

* Corresponding author. Tel.: +81 43 290 3114; fax: +81 43 290 3403.
E-mail address: hhayashi@faculty.chiba-u.jp (H. Hayashi).

0968-0896/$ - see front matter © 2013 Elsevier Ltd. All rights reserved.
http://dx.doi.org/10.1016/j.bmc.2013.12.026

the ideal candidate as an NIR-fluorescence imaging probe. For instance, Jeong et al. have reported the modification of liposome via mannosylation of phospholipid and the lymph node imaging by ICG contained in the modified liposome.[74] Proulx et al. have reported on the high stability and high sensitivity of LP-ICG for NIR-fluorescence imaging of lymph nodes in vivo by its administration to lower extremities of mice.[75] However, LP-ICG has still shown to accumulate in not only a first draining lymph node but also a second-tier node in the lower extremities of mice. We hypothesized that ICG can leak out from the liposomal membrane in vivo; thus, we synthesized a novel ICG, which is more hydrophobic than conventional ICG, by substitution of one sulfonate groups of the ICG with an alkyl chain (ICG-Cn; n = 4, 6, 8, 10, and 18). We examined the spectral properties of ICG-Cn in both an organic solution and a liposomal dispersion, and we visualized the lymph nodes in the lower extremities of mice by using liposomally formulated ICG-Cn (LP-ICG-Cn) as well as LP-ICG and ICG under a NIR-fluorescence imaging system.

2. Material and methods

2.1. Synthesis of 18-(2-((1*E*,3*E*,5*E*,7*E*)-7-(1,1-dimethyl-3-butyl-1*H*-benzo[*e*]indol-2(3*H*)-ilydene)hepta-1,3,5-trienyl)-1,1-dimethyl-1*H*-benzo[*e*]indolium-3-yl)octadecane-1-sulforic acid (ICG-C18) and other ICG-Cn (n = 4, 6, 8, and 10)

The process of ICG-C18 synthesis follows the conventional processes for synthesis of ICG and other ICG derivatives reported elsewhere (Scheme 2).[45,56,77] 2,3,3-Trimethyl-4,5-benzo-3*H*-indole (3.1 g, 15 mmol) and 1,4-butane sultone (2.1 g, 15 mmol) were mixed in a round-bottomed flask (25 mL) under a nitrogen atmosphere, and the reaction solution was stirred at 80 °C for 4 h and then cooled at room temperature. By addition of acetone to the reaction mixture, the residue was dissolved, and the product was crystallized. The reaction product, 2,3,3-trimethyl-1-(sulfobutyl)-4,5-benzoindolium inner salt, was separated by filtration and rinsed with acetone. The product was obtained as a gray crystal (1.17 g, 23%).

A reaction mixture of the gray crystal (1.04 g, 3.0 mmol) and glutaconaldehyde dianil hydrogen chloride salt (0.94 g, 3.3 mmol) was stirred at 120 °C for 1 h and then cooled at room temperature to crystallize the product, 2-(6-acetanilido-1,3,5-hexatrienyl)-3,3-dimethyl-1-(sulfobutyl)-4,5-benzo[*e*]indolium inner salt. The salt was then separated by filtration and rinsed with acetone. The product was obtained as a dark purple crystal (0.97 g, 58%).

A 2-butanone solution (40 mL) of 2,3,3-trimethyl-4,5-benzo-3*H*-indole (8.4 g, 40 mmol) and 1-iodooctadecane (16.8 g, 44 mmol) was stirred in a round-bottomed flask (100 mL) at 70 °C for 18 h and then cooled at room temperature. After addition of ethyl acetate (40 mL) to crystallize the product, 1-octadecyl-2,3,3-trimethyl-4,5-benzo[*e*]indolium iodide, was separated by filtration and rinsed twice with ethyl acetate. The product was obtained as a gray crystal (4.4 g, 19%).

Finally, a pyridine solution (16 mL) of the indolium inner salt (1.58 g, 3.0 mmol) and the indolium iodide (1.77 g, 3.0 mmol) was stirred at 50 °C for 1 h under a nitrogen atmosphere. After cooling at room temperature and addition of distilled water (40 mL), the crystallized product was separated by filtration and dissolved in ethyl acetate. The residue of the solution was filtered and recrystallized in 40 mL of chloroform/ethyl acetate (1/1, volume ratio), and the product was obtained as a dark green crystal (1.39 g, 53%). The other ICG derivatives: ICG-Cn (n = 4, 6, 8, and 10), with different alkyl chains from ICG-C18, were synthesized using the same procedure and the corresponding indolium salts. Yields of 46% (ICG-C4), 59% (ICG-C6), 57% (ICG-C8), and 44% (ICG-C10) were obtained.

The ^{1}H NMR spectra of ICG-Cn (n = 4, 6, 8, 10, and 18) were run at 300 MHz in DMSO-d_6 by using a Lambda-300 NMR spectrometer (JEOL, Tokyo, Japan). The infrared spectra of these compounds were recorded on an IRPrestige-21 spectrometer (Shimadzu, Kyoto, Japan) in the range of 4000–400 cm^{-1} using potassium bromide pellets. Electron spray ionization mass spectroscopy (ESI-MS) was examined using LCMS-2010EV (Shimadzu, Kyoto, Japan).

ICG-C4: ^{1}H NMR (300 MHz, DMSO-d_6): δ 0.94 (t, 3H, J = 7.0 Hz); 1.43 (m, 2H); 1.79 (m, 18H); 2.54 (m, 2H); 4.20 (m, 4H); 6.36 (d, 1H, J = 13.8 Hz); 6.57 (m, 3H); 7.47 (m, 2H); 7.63 (m, 3H); 7.78 (m, 2H); 7.99 (m, 6H); 8.22 (d, 2H, J = 8.5 Hz). IR (KBr, cm^{-1}): 3051, 2930, 2871, 1630, 1418, 1310, 1138. ESI-MS (methanol/acetonitrile = 1:1): m/z = 673 [M+H$^+$].

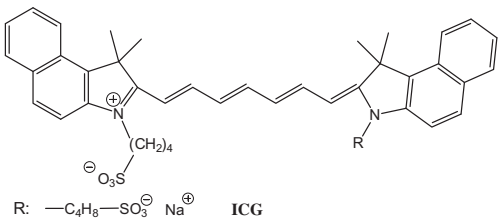

R:		
	—C_4H_8—SO_3^- Na^+	**ICG**
	—C_4H_9	**ICG-C4**
	—C_6H_{13}	**ICG-C6**
	—C_8H_{17}	**ICG-C8**
	—$C_{10}H_{21}$	**ICG-C10**
	—$C_{18}H_{37}$	**ICG-C18**

Scheme 1. Structures of ICG and ICG-Cn (n = 4, 6, 8, 10, and 18).

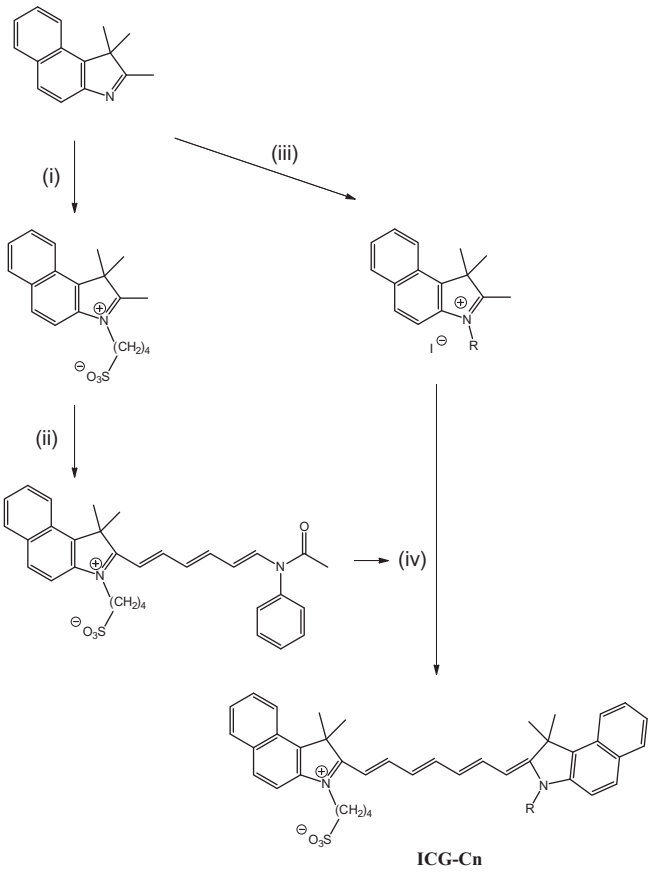

Scheme 2. Synthesis of ICG-Cn: (i) 1,4-butane sultone, (ii) glutacon-aldehyde dianil hydrogen chloride salt, (iii) $C_nH_{2n+1}I$ (n = 4, 6, 8, 10, and 18), 2-butanone, and (iv) pyridine.

ICG-C6: ^{1}H NMR (300 MHz, DMSO-d_6): δ 0.85 (t, 3H, J = 7.0 Hz); 1.20–1.45 (m, 6H); 1.65–2.0 (m, 18H); 2.42–2.65 (m, 2H); 4.20 (quintet, 4H); 6.37 (d, 1H, J = 12.7 Hz); 6.61 (m, 3H); 7.47 (m, 2H); 7.59–7.70 (m, 3H); 7.72–7.85 (m, 2H); 7.90–8.07 (m, 6H); 8.22 (d, 2H, J = 8.5 Hz). IR (KBr, cm^{-1}): 3051, 2930, 1630, 1508, 1417, 1354, 1094, 924, 665. ESI-MS (methanol/acetonitrile = 1:1): m/z = 701 [M+H$^+$].

ICG-C8: ^{1}H NMR (300 MHz, DMSO-d_6): δ 0.82 (t, 3H, J = 6.6 Hz); 1.32 (m, 10H); 1.79 (m, 18H); 2.54 (m, 2H); 4.20 (m, 4H); 6.36 (d, 1H, J = 13.7 Hz); 6.57 (m, 3H); 7.48 (m, 2H); 7.64 (m, 3H); 7.78 (m, 2H); 7.99 (m, 6H); 8.22 (d, 2H, J = 8.6 Hz). IR (KBr, cm^{-1}): 3051, 2928, 2855, 1624, 1418, 1310, 1138. ESI-MS (methanol/acetonitrile = 1:1): m/z = 729 [M+H$^+$].

ICG-C10: ^{1}H NMR (300 MHz, DMSO-d_6): δ 0.81 (t, 3H, J = 6.7 Hz); 1.32 (m, 14H); 1.80 (m, 18H); 2.54 (m, 2H); 4.20 (m, 4H); 6.36 (d, 1H, J = 13.7 Hz); 6.57 (m, 3H); 7.47 (m, 2H); 7.63 (m, 3H); 7.78 (m, 2H); 7.99 (m, 6H); 8.22 (d, 2H, J = 8.6 Hz). IR (KBr, cm^{-1}): 3060, 2924, 2853, 1635, 1418, 1310, 1138. ESI-MS (methanol/acetonitrile = 1:1): m/z = 757 [M+H$^+$].

ICG-C18: ^{1}H NMR (300 MHz, DMSO-d_6): δ 0.82 (t, 3H, J = 6.6 Hz); 1.30 (m, 30H); 1.80 (m, 18H); 2.54 (m, 2H); 4.20 (m, 4H); 6.36 (d, 1H, J = 13.8 Hz); 6.56 (m, 3H); 7.47 (m, 2H); 7.63 (m, 3H); 7.77 (m, 2H); 7.99 (m, 6H); 8.22 (d, 2H, J = 8.1 Hz). IR (KBr, cm^{-1}): 3040, 2922, 2851, 1624, 1414, 1310, 1136. ESI-MS (methanol/acetonitrile = 1:1): m/z = 869 [M+H$^+$].

2.2. Preparation of LP-ICG and LP-ICG-Cn

1,2-Dioleoyl-3-sn-glycero-phosphocholine (10.0 mM; NOF, Tokyo, Japan), cholesterol (1.0 mM; NOF), phosphatidylethanolamine-*N*-methoxy-polyethylene glycol(5000)-dioleoyl-glycero ammonium salt (5.0×10^{-1} mM; NOF), and ICG or ICG-Cn were dissolved in an mixed organic solvent of chloroform/methanol (9:1, volume ratio). A thin lipid film was formed by removal of the solvent under reduced pressure. After addition of the glucose isotonic solution (5% [w/v]) at room temperature, the liposomal dispersion was filtered through a 0.4-μm pore filter made of polycarbonate (Millipore, MA, USA). The liposomal size distribution was determined by dynamic light scattering measurements (UPA-UT151; NIKKISO, Tokyo, Japan).

To determine the ratio of ICG or ICG-C18 leaking from the liposomes, we used a preparative gel permeable chromatographic column (PD-10; GE Healthcare Bio-Sciences AB, Uppsala, Sweden) and measured the absorbance of the obtained fraction (200 μL) separated from the liposomal dispersion using an absorbance spectrophotometer at 805 nm (UV-1800, Shimadzu, Kyoto, Japan).

2.3. Absorbance and fluorescence spectroscopy

The absorbance spectrophotometer was also used to measure the absorption spectra of ICG and ICG-Cn dissolved in a spectroscopic grade ethanol (Kanto, Tokyo, Japan). Excitation and emission spectra of ICG, ICG-Cn, LP-ICG, and LP-ICG-Cn were obtained using a fluorospectrometer (FP-6600; JASCO, Japan). Spectroscopic grade chloroform (Kanto) was used as the solvent for ICG and ICG-Cn.

2.4. NIR-fluorescence imaging

To obtain the NIR-fluorescence image of the liposome dispersions after injection into the mice, a noninvasive fluorescence imaging system (IVIS Lumina II; Caliper, MA, USA) was used with an XFL-HR Fluorescence Filter Option High Range (720–840 nm) detection filter. The fluorescence photons from each sample were counted and statistically compared using a t-test, with statistical significance set at $p < 0.05$.

2.5. Injection of ICG solution or liposomal dispersion into footpads of mice

Six-week-old male KSN mice were purchased from Japan SLC, Inc. (Shizuoka, Japan) and kept under specific pathogen-free and humane conditions in the animal care facility of the Research Center for Frontier Medical Engineering, Chiba University, Japan. After anesthetization by intraperitoneal injection of pentobarbital (40 mg/kg; Dainippon Sumitomo Pharma, Japan), 10 μL of ICG solution, LP-ICG, or LP-ICG-C18 dispersion was injected into a rear footpad of the mouse. The stage beneath the mouse was kept at 30 °C during the imaging. The animal experiment protocol was reviewed and approved by the Institutional Animal Care and Use Committee of Animal Experimentation, Chiba University.

2.6. Single-dose toxicity assay of LP-ICG-C18

All animal procedures were approved by Chiba University and the Kamakura Techno-Science Inc. Institutional Animal Care and Use Committee. Six-week-old male (SPF, Crl:CD [SD]) rats were purchased from Charles River Laboratories Japan (Kanagawa, Japan) and housed separately under specific pathogen-free and

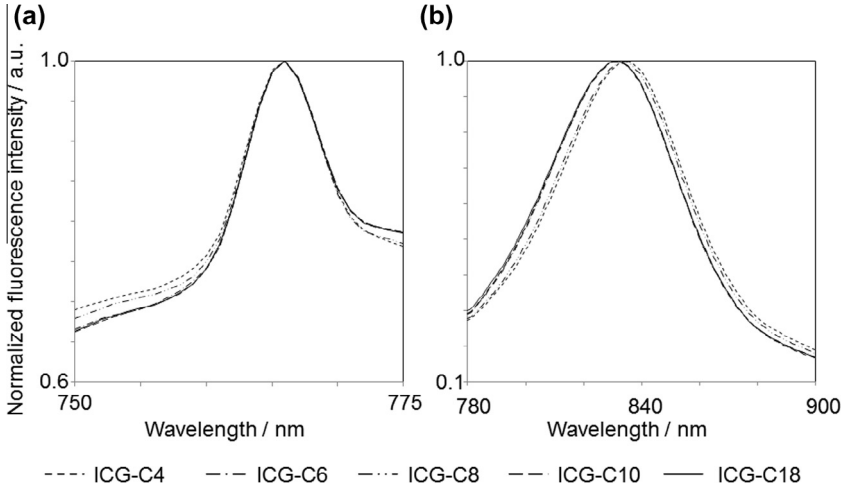

Figure 1. Fluorescence excitation (a) and emission (b) spectra of ICG-Cn dissolved in chloroform (32 μM).

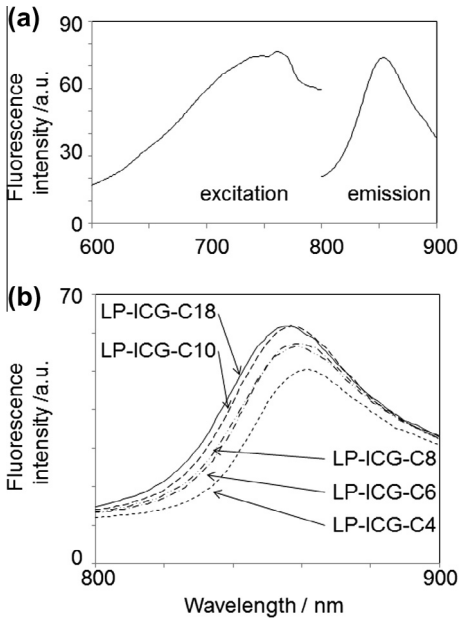

Figure 2. (a) Fluorescence excitation and emission spectra of LP-ICG-C18. (b) Emission spectra of LP-ICG-Cn.

humane conditions. A group of five rats was orally administered LP-ICG-C18 (10 mL/kg) once a day. Another group of five rats was intravenously administered LP-ICG-C18 (5 mL/kg) once a day. As a reference group, five rats were administered saline, with the same volume and frequency as both the treatment groups. The body weights of the rats were monitored for 15 days.

3. Results and discussion

3.1. Fluorescence characteristics of ICG-Cn

ICG, which is a water-soluble carbocyanine dye that has two sulfonate groups (Scheme 1), has drawn much attention as a clinically useful NIR-fluorescent molecule. To develop an ICG-based NIR-fluorescent probe for SLN imaging, we synthesized alkylated ICG molecules (ICG-Cn, $n = 4$, 6, 8, 10, and 18), which are expected to be more hydrophobic than ICG (see Section 2). Briefly, 2 types of substituted 2,3,3-trimethyl-4,5-benzo-3*H*-indol were coupled using glutaconaldehyde dianil hydrogen chloride (Scheme 2); the yields of all ICG-Cn compounds in the coupling reaction were greater than 40%, which are acceptable as the previous report.[45] To clarify the fluorescence properties of ICG-Cn ($n = 4$, 6, 8, 10, and 18), we performed the absorbance and fluorescence spectroscopy on ICG and ICG-Cn. The maximum absorbance wavelengths of ICG-Cn in ethanol (32 μM) were in the range of 787–788 nm, which is similar to that of ICG. The molar absorbance coefficient of ICG was 1.47×10^5 and those of ICG-Cn were in the range of $1.24–2.63 \times 10^5$. The difference of molar absorbance coefficients among ICG-Cn is probably due to the effect of solvent (ethanol) to the excitation state or molecular interaction of ICG-Cn. However, we imply that substitution of the sulfonate group with an alkyl chain scarcely affect the molecular energy level of the carbocyanine chromophore. The excitation/emission spectra of ICG-Cn in chloroform (32 μM) are shown in Figure 1. The maximum wavelength of excitation was 766 nm for all dyes, and the maximum wavelength of emission was in the range of 831–834 nm; these wavelength are almost identical to those of ICG in chloroform.

ICG dissolved in aqueous solution has a maximum excitation wavelength of 780 nm and a maximum emission wavelength of 810 nm.[41,42,55,58,59] In the presence of lipoproteins,[42] phospholipids,[60,74,75] or polymer colloidal particles,[60,64] the maximum excitation is shifted to over 800 nm, and the maximum emission reaches over 810 nm.[53,57,68,74,75] Since the absorbance and fluorescence properties of ICG-Cn compounds were the same as those of ICG, ICG-Cn compounds have potential for liposome formulation as the NIR-fluorescent probes. Therefore, we assessed the fluorescence spectra of liposomally formulated ICG (LP-ICG) and ICG-Cn (LP-ICG-Cn) after filtration of liposomes with a 0.4-μm pore filter. The spectra of the fluorescence excitation/emission of LP-ICG-C18 are shown in Figure 2a. The spectra of liposomal dispersions containing ICG-Cn ($n = 4$, 6, 8, and 10) is similar to that shown in

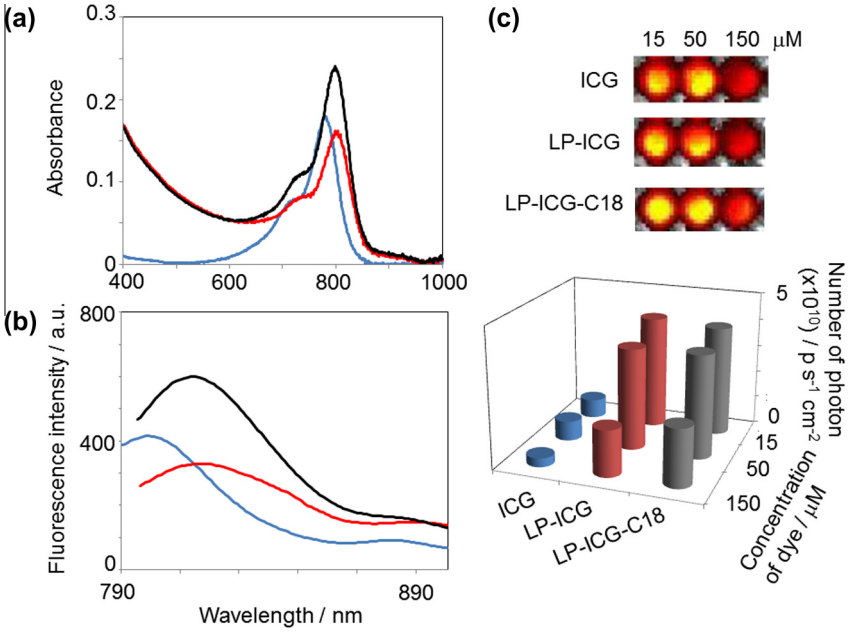

Figure 3. (a) Absorbance spectra and (b) fluorescence emission spectra of ICG solution (blue), LP-ICG (red), and LP-ICG-C18 (black) respectively. The wavelength of excitation is 771 nm for ICG solution and 773 nm for both LP-ICG and LP-ICG-C18. (c) Histogram of average number of photons of ICG solution (blue), LP-ICG (red), and LP-ICG-C18 (gray) detected by the quantitative NIR-fluorescence imaging system (each NIR-fluorescence image is also shown).

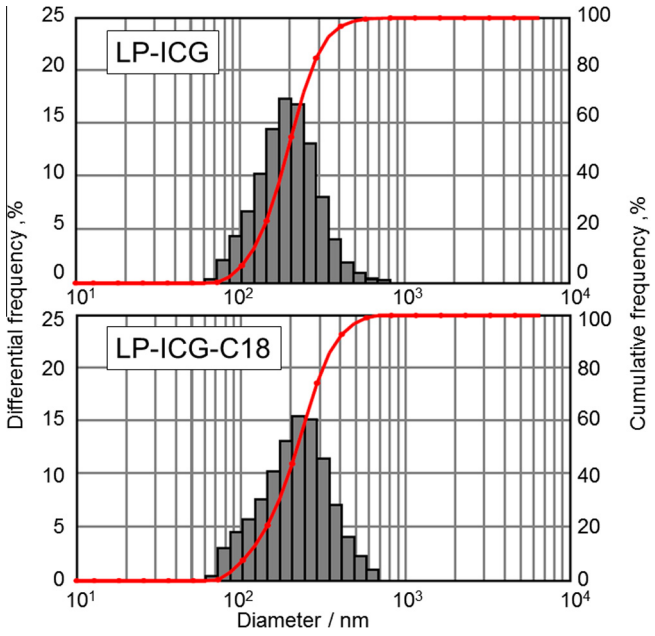

Figure 4. Size distribution of LP-ICG and LP-ICG-C18. Gray bars represent the differential frequency and the red line indicates the cumulative frequency.

Figure 2a, and it should be noted that these excitation spectra typically exhibit a wide peak with a width of approximately 100 nm, whereas the emission spectra show a narrow peak. This implies that several energy states of ICG-Cn exist when ICG-Cn compounds are incorporated into liposomal membranes. The carbocyanine chromophore is probably located in several different regions tangential to the membrane, such as the hydrophobic region of the condensed bushes of the alkyl chains of the lipids, the electric bilayer region comprising the polar heads of the lipids, and the hydrophilic and polyethylene glycol-rich region above the liposome surface. In contrast, the fluorescence emission spectra of LP-ICG-Cn (n = 4, 6, 8, 10, and 18) are narrow in the range of 850–865 nm when they are excited at 738 nm (Fig. 2b). The peak wavelength of the fluorescence emission exhibits a blueshift, and the fluorescence intensity increases as the carbon number of the substituted alkyl chain of the ICG derivatives increases. This probably results from the shift in location of the carbocyanine chromophore from the vicinity of the liposome surface into the hydrophobic region, which prevents photobleaching and redshift[55] as the carbon number of the substituted alkyl chain increases. We thus conclude that substitution of the sulfonate group of ICG with an alkyl chain results in both an increase in the binding properties of the carbocyanine chromophore and reinforcement of its fluorescence compared to ICG.

3.2. In vitro and in vivo NIR-fluorescence imaging of LP-ICG and LP-ICG-C18

Based on the properties of ICG-Cn and LP-ICG-Cn, we examined NIR-fluorescence imaging with LP-ICG-C18, because the fluorescence intensity of LP-ICG-C18 was higher than those of the other LP-ICG-Cn compounds (n = 4, 6, 8, and 10). When the absorbance and fluorescence intensities of an ICG aqueous solution (glucose isotopic solution; concentration of ICG = 0.03 mM), LP-ICG, and LP-ICG-C18 were measured, the intensity of LP-ICG-C18 was found to be higher than that of the ICG solution and LP-ICG (Fig. 3a and b). By changing the concentration of ICG-C18 in the initially

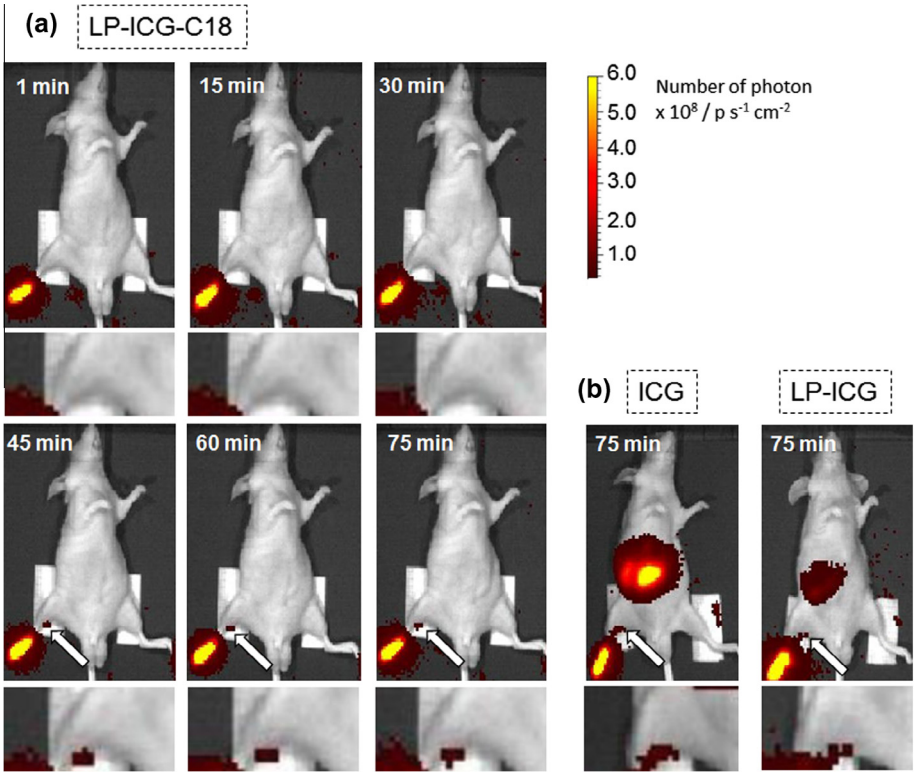

Figure 5. (a) Time course of NIR-fluorescence images of mice in which a footpad was injected with 10 mL of LP-ICG-C18. White arrows indicate detection of the NIR-fluorescent spot at the location of the popliteal lymph node. (b) Reference experiment data using ICG aqueous solution and LP-ICG. Not only the popliteal lymph node but also the liver fluoresces after 30 min, and the intensity was maintained over 1 h. The enlarged views for the popliteal lymph node of each mouse were attached below the corresponding NIR-fluorescence images.

prepared organic solution of the lipid mixture, we measured LP-ICG-C18 fluorescence with a quantitative NIR-fluorescence imaging system.[78] We found that the fluorescence intensities of LP-ICG-C18 and LP-ICG were statistically similar and larger than that of the ICG aqueous solution at the concentrations of 15 and 50 μM (Fig. 3c). This is probably because photobleaching of the carbocyanine chromophore occurs in the aggregation of the ICG solution, and ICG and ICG-C18 can merge with phospholipids in liposomes, preventing such photobleaching. At the concentration of 150 μM, the number of fluorescence photons emitted from LP-ICG-C18 was greater than that emitted of LP-ICG. Assuming that the size distribution of LP-ICG and LP-ICG-C18 is the same, this is probably because the carbocyanine chromophore of ICG is saturated and aggregated in the liposomal membrane, whereas ICG-C18 is likely merged in the membrane due to the substituted alkyl chain.

We thus measured the size distribution of LP-ICG and LP-ICG-C18 after filtration and the leak of ICG and ICG-C18 from the liposome. Figure 4 shows the size distribution of LP-ICG-C18 and LP-ICG after filtration through a 0.4-μm pore filter; we found that the hydrodynamic diameter of LP-ICG-C18 was 235 ± 101 nm (average ± standard deviation), which is almost same as that of LP-ICG (209 ± 79 nm). Using a preparative gel-permeable chromatographic column and absorbance spectrophotometer, we measured the fraction of leaked ICG or ICG-C18 separated from the liposomal dispersion after the filtration. We found that the leaked fraction of ICG-C18, as well as that of ICG, was less than 0.5% (see Supplementary material). Therefore, we deduced that the influence of ICG-C18 on liposomal properties is not different from that of ICG and that ICG-C18 is more likely to be mono-dispersed and to fluoresce in the liposomal membrane than ICG at relatively high concentrations.

To examine LP-ICG-C18 for use in NIR-imaging in vivo, we injected 10 μL of LP-ICG-C18, LP-ICG, or aqueous ICG into the rear footpads of anesthetized mice and observed them using the NIR-fluorescence imaging system. As shown in Figure 5, after injection of the ICG solution, fluorescence detected in not only the popliteal lymph node but also in the liver. In the mouse injected with LP-ICG, the popliteal lymph node and the liver appeared fluorescent after 30 min. However, in the case of LP-ICG-C18, only the popliteal lymph node appeared fluorescent, even after more than 1 h. As reviewed by Keshtgar and Ell,[79] the ideal colloidal probes for imaging the sentinel lymph node satisfy several requirements including long-term retention in the sentinel lymph node and high stability for sustaining the volume therein. The results observed in the case of ICG or LP-ICG were probably due to the influence of spontaneous pressure from interstitial fluid onto the lymph nodes or from macrophage activity that causes ICG or LP-ICG to leak from lymph nodes and accumulate in the liver, whereas LP-ICG-C18 is not affected by these factors and so was only observed in the popliteal lymph node. Although the size distribution and composition ratio of lipids were almost the same between LP-ICG and LP-ICG-C18, this is probably because the hydrophobic part of ICG-C18 reinforces liposomal membrane self-assembly and stiffness.[80,81] Moreover, we observed no significant toxicity of LP-ICG-C18 to mice administered with LP-ICG-C18 via both oral and intravenous routes (see Supplementary material). Although further distribution analyses such as using tumor-bearing mouse models are required, LP-ICG-C18 is expected to play an important role in decreasing the false-negative rate of SLN biopsy in pre-clinical or clinical use.[82,83]

4. Conclusions

The purpose of the present study was to develop LP-ICG-Cn that would be useful as NIR-fluorescence colloidal probes. LP-ICG-C18 gave brilliant fluorescence images under the NIR-fluorescence imaging system in vitro and in vivo and remained in only the popliteal lymph node in the mouse-footpad injection experiment. The toxicity assay revealed that administration of LP-ICG-C18 via both oral and intravenous routes had no effect on the mice. Although further analyses are required, these results indicated that LP-ICG-C18 would be potentially powerful for use in noninvasive NIR-bioimaging for SLNs.[60–62,84,85]

Acknowledgments

The single-dose toxicity assay of LP-ICG-C18 was performed at Kamakura Techno-Science Inc. (Kanagawa, Japan). This work was partially supported by Grants-in-Aid for Scientific Research from the Ministry of Education, Culture, Sports, Science and Technology in Japan (No. 21790238 to A.S., No. 22501022 to Y.T., No. 23750078 to T.T. and No. 21591693 to H.H.) and a Research Grant from the Futaba Electronics Memorial Foundation (to A.S. and Y.T.).

Supplementary data

Supplementary data (^{1}H NMR spectra, IR spectra, MS spectra, and HPLC charts for each ICG-Cn, gel-filtration chromatography charts of LP-ICG and LP-ICG-C18, and the results of single-dose toxicity assay using LP-ICG-C18) associated with this article can be found, in the online version, at http://dx.doi.org/10.1016/j.bmc.2013.12.026.

References and notes

1. Warner, G. T.; Oliver, R. *Phys. Med. Biol.* **1966**, *11*, 83.
2. Earle, M.; Chapman, M. D. *J. Am. Med. Assoc.* **1983**, *250*, 2042.
3. Schwochau, K. *Technetium: Chemistry and Radiopharmaceutical Applications*; Wiley-VCH: Weinheim, 2000.
4. Bailey, D. L.; Townsend, D. W.; Valk, P. E.; Maisey, M. N. *Positron Emission Tomography*; Springer-Verlag: London, 2005.
5. Hill, C. R. *Br. J. Radiol.* **1976**, *49*, 238.
6. Wells, P. N. T. *Rep. Prog. Phys.* **1999**, *62*, 671.
7. Azhari, H. *Basic of Biomedical Ultrasound for Engineers*; John Wiley & Sons Inc: New Jersey, 2010.
8. Tilcock, C. *Adv. Drug Delivery Rev.* **1999**, *37*, 33.
9. Torchilin, V. P. *Nat. Rev.* **2005**, *4*, 145.
10. McRobbie, D. W.; Moore, E. A.; Graves, M. J.; Prince, M. R. *MRI from Picture to Proton*; Cambridge University Press: New York, 2006.
11. Farkas, D. L.; Du, C.; Fisher, G. W.; Lau, C.; Niu, W.; Wachman, E. S.; Levenson, R. M. *Comput. Med. Imaging Graphics* **1998**, *22*, 89.
12. Frangioni, J. V. *Curr. Opin. Chem. Biol.* **2003**, *7*, 626.
13. Petrovsky, A.; Schellenberger, E.; Josephson, L.; Weissleder, R.; Bogdanov, A., Jr. *Cancer Res.* **2003**, *63*, 1936.
14. Ntziachristos, V.; Bremer, C.; Weissleder, R. *Eur. Radiol.* **2003**, *13*, 195.
15. Chen, Y.; Intes, X.; Chance, B. *Biomed. Instrum. Technol.* **2005**, *39*, 75.
16. Koo, V.; Hamilton, P. W.; Williamson, K. *Anal. Cell Pathol.* **2006**, *28*, 127.
17. Rao, J.; Dragulescu-Andrasi, A.; Yao, H. *Curr. Opin. Biotechnol.* **2007**, *18*, 17.
18. Lim, C.-K.; Lee, Y.-D.; Na, J.; Oh, J. M.; Her, S.; Kim, K.; Choi, K.; Kim, S.; Kwon, I. C. *Adv. Funct. Mater.* **2010**, *20*, 2644.
19. *Topics in Fluorescence Spectroscopy*; Lakowicz, J. R., Ed.; Springer: New York, 1994; Vol. 4..
20. Cherukuri, P.; Bachilo, S. M.; Litovsky, S. H.; Weisman, R. B. *J. Am. Chem. Soc.* **2004**, *126*, 15638.
21. Ohnishi, S.; Lomnes, S. J.; Laurence, R. G.; Gogbashian, A.; Mariani, G.; Frangioni, J. V. *Mol. Imaging* **2005**, *4*, 172.
22. Sasaki, E.; Kojima, H.; Nishimatsu, H.; Urano, Y.; Kikuchi, K.; Hirata, Y.; Nagano, T. *J. Am. Chem. Soc.* **2005**, *127*, 3684.
23. Amiot, C. L.; Xu, S.; Liang, S.; Pan, L.; Zhao, J. X. *Sensors* **2008**, *8*, 3082.
24. Zhang, Z.; Berezin, M. Y.; Kao, J. L. F.; d'Avignon, A.; Bai, M.; Achilefu, S. *Angew. Chem.* **2008**, *120*, 3640.
25. Troyan, S. L.; Kianzad, V.; Gibbs-Strauss, S. L.; Gioux, S.; Matui, A.; Oketokoun, R.; Ngo, L.; Khamene, A.; Azar, F.; Frangioni, J. V. *Ann. Surg. Oncol.* **2009**, *16*, 2943.
26. Kundu, K.; Knight, S. F.; Willet, N.; Lee, S.; Taylor, W. R.; Murthy, N. *Angew. Chem., Int. Ed.* **2009**, *48*, 299.
27. Qian, G.; Wang, Z. Y. *Chem. Asian J.* **2010**, *5*, 1006.
28. Kamat, N. P.; Liao, Z.; Moses, L. E.; Rawson, J.; Therien, M. J.; Dmochowski, I. J.; Hammer, D. A. *Proc. Natl. Acad. Sci. U.S.A.* **2011**, *108*, 13984.
29. Weissleder, R.; Tung, C.-H.; Mahmood, U.; Bogdanov, A., Jr. *Nat. Biotechnol.* **1999**, *17*, 375.

30. Kim, S.; Lim, Y. T.; Soltesz, E. G.; DeGrand, A. M.; Lee, J.; Nakayama, A.; Parker, J. A.; Mihaljevic, T.; Laurence, R. G.; Dor, D. M.; Cohn, L. H.; Bawendi, M. G.; Frangioni, J. V. *Nat. Biotechnol.* **2004**, *22*, 93.
31. Barone, P. W.; Baik, S.; Heller, D. A.; Strano, M. *Nat. Mater.* **2005**, *4*, 86.
32. Ghoroghchian, P. P.; Frail, P. R.; Susumu, K.; Blessington, D.; Brannan, A. K.; Bates, F. S.; Chance, B.; Hammer, D. A.; Therien, M. J. *Proc. Natl. Acad. Sci. U.S.A.* **2005**, *102*, 2922.
33. Rhyner, M. N.; Smith, A. M.; Gao, X.; Mao, H.; Yang, L.; Nie, S. *Nanomedicine* **2006**, *1*, 209.
34. le Masne de Chermont, Q.; Chanéac, C.; Seguin, J.; Pellé, F.; Maítrejean, S.; Jolivet, J.-P.; Gourier, D.; Bessodes, M.; Scherman, D. *Proc. Natl. Acad. Sci. U.S.A.* **2007**, *104*, 9266.
35. Antinoğlu, E. İ.; Russin, T. J.; Kaiser, J. M.; Barth, B. M.; Eklund, P. C.; Kester, M.; Adair, J. H. *ACS Nano* **2008**, *2*, 2075.
36. Saad, M.; Garbuzenko, O. B.; Ber, E.; Chandna, P.; Khandare, J. J.; Pozharov, V. P.; Minko, T. *J. Controlled Release* **2008**, *130*, 107.
37. Bharali, D. J.; Khalil, M.; Gurbuz, M.; Simone, T. M.; Mousa, S. A. *Int. J. Nanomed.* **2009**, *4*, 1.
38. He, X.; Wang, K.; Chen, Z. *Interdiscip. Rev. Nanomed. Nanobiotechnol.* **2010**, *2*, 349.
39. Mohan, N.; Tzeng, Y.-K.; Yang, L.; Chen, Y.-Y.; Hui, Y. Y.; Fang, X.-Y.; Chang, H.-C. *Adv. Mater.* **2010**, *22*, 843.
40. Zhou, F.; Wu, S.; Wu, B.; Chen, W. R.; Xing, D. *Small* **2011**, *7*, 2727.
41. Cherrick, G. R.; Stein, S. W.; Leevy, C. M.; Davidson, C. S. *J. Clin. Invest.* **1960**, *39*, 592.
42. Yoneya, S.; Saito, T.; Komatsu, Y.; Koyama, I.; Takahashi, K.; Duvoll-Young, J. *Invest. Ophthalmol. Vis. Sci.* **1998**, *39*, 1286.
43. Schaafsma, B. E.; Mieog, J. S.; Hutteman, M.; van der Vorst, J. R.; Kuppen, P. J.; Löwik, C. W.; Frangioni, J. V.; van der Velde, C. J.; Vahrmeijer, A. L. *J. Surg. Oncol.* **2011**, *104*, 323.
44. Vinegoni, C.; Bontnaru, I.; Aikawa, E.; Calfon, M. A.; Iwamoto, Y.; Folco, E. J.; Ntziachristos, V.; Weissleder, R.; Libby, P.; Jaffer, F. A. *Sci. Transl. Med.* **2011**, *3*(84r), a45.
45. Narayanan, N.; Patonay, G. *J. Org. Chem.* **1995**, *60*, 2391.
46. Flanagan, J. H., Jr.; Khan, S. H.; Menchen, S.; Soper, S. A.; Hammer, R. P. *Bioconjugate Chem.* **1997**, *8*, 751.
47. Sevick-Muraca, E.; Houston, J. P.; Gurfinkel, M. *Curr. Opin. Chem. Biol.* **2002**, *6*, 642.
48. Masotti, A.; Vicennati, P.; Boschi, F.; Calderan, L.; Sbarbati, A.; Ortaggi, G. *Bioconjugate Chem.* **2008**, *19*, 983.
49. Watanabe, M.; Tsunoda, A.; Narita, K.; Kusano, M.; Miwa, M. *Surg. Today* **2009**, *39*, 214.
50. Texier, I.; Goutayer, M.; Silva, A. D.; Guyon, L.; Djaker, N.; Josserand, V.; Neumann, E.; Bibette, J.; Vinet, F. *J. Biomed. Opt.* **2009**, *14*, 054005.
51. Milej, D.; Kacprzak, M.; Żołek, N.; Sawosz, P.; Gereca, A.; Maniewski, R.; Liebert, A. *Opto-Electron. Rev.* **2010**, *18*, 208.
52. Buckle, T.; van Leeuwen, A. C.; Chin, P. T. K.; Janssen, H.; Muller, S. H.; Jonkers, J.; van Leeuwen, F. W. B. *Nanotechnology* **2010**, *21*, 355101.
53. Zheng, X.; Xing, D.; Zhou, F.; Wu, B.; Chen, W. R. *Mol. Pharm.* **2011**, *8*, 447.
54. Ornelas, C.; Lodescar, R.; Durandin, A.; Canary, J. W.; Pennell, R.; Liebes, L. F.; Weck, M. *Chem. Eur. J.* **2011**, *17*, 3619.
55. Zhu, R.; Lü, R.; Yu, A. *Chin. J. Chem.* **2011**, *29*, 405.
56. Choi, H. S.; Nasr, K.; Alyabyev, S.; Feith, D.; Lee, J. H.; Kim, S. H.; Ashitate, Y.; Hyun, H.; Patonay, G.; Strekowski, L.; Henary, M.; Frangioni, J. V. *Angew. Chem., Int. Ed.* **2011**, *50*, 6258.
57. Noh, Y.-W.; Park, H. S.; Sung, M.-H.; Lim, Y. T. *Biomaterials* **2011**, *32*, 6551.
58. Saxena, V.; Sadoqi, M.; Shao, J. *J. Pharm. Sci.* **2003**, *92*, 2090.
59. Dzurinko, V. L.; Gurwood, A. S.; Price, J. R. *Optometry* **2004**, *75*, 743.
60. Kitai, T.; Inomoto, T.; Miwa, M.; Shikayama, T. *Breast Cancer* **2005**, *12*, 211.
61. Fujiwara, M.; Mizukami, T.; Suzuki, A.; Fukamizu, H. *J. Plast. Reconstr. Aesthet. Surg.* **2009**, *62*, e373.
62. Kusano, M.; Tajima, Y.; Yamazaki, K.; Kato, M.; Watanabe, M.; Miwa, M. *Dig. Surg.* **2008**, *25*, 103.
63. Alford, R.; Simpson, H. M.; Duberman, J.; Hill, G. C.; Ogawa, M.; Regino, C.; Kobayashi, H.; Choyke, P. L. *J. Mol. Imaging* **2009**, *8*, 341.
64. Hirano, A.; Kamimura, M.; Ogura, K.; Kim, N.; Hattori, A.; Setoguchi, Y.; Okubo, F.; Inoue, H.; Miyamoto, R.; Kinoshita, J.; Fujibayashi, M.; Shimizu, T. *Ann. Surg. Oncol.* **2012**, *19*, 4112.
65. Namikawa, K.; Yamazaki, N. *Eur. J. Dermatol.* **2011**, *21*, 184.
66. Tajima, Y.; Murakami, M.; Yamazaki, K.; Masuda, Y.; Kato, M.; Sato, A.; Goto, S.; Otsuka, K.; Kato, T.; Kusano, M. *Ann. Surg. Oncol.* **2010**, *17*, 1787.
67. Yamashita, S.; Tokuishi, K.; Anami, K.; Miyawaki, M.; Moroga, T.; Kamei, M.; Suehiro, S.; Ono, K.; Takeno, S.; Chujo, M.; Yamamoto, S.; Kawahara, K. *J. Thorac. Cardiovasc. Surg.* **2011**, *141*, 141.
68. Mordon, S.; Desmettre, T.; Devoisselle, J. M.; Soulie, S. *Lasers Surg. Med.* **1996**, *18*, 265.
69. Woodle, M. C.; Storm, G. *Long Circulating Liposomes*; Springer: Berlin, 1998.
70. Toledano, H.; Edrei, R.; Kimel, S. *J. Photochem. Photobiol., B* **1998**, *42*, 20.
71. Torchilin, V. P.; Weissig, V. *Liposomes: A Practical Approach*; Oxford University Press: Oxford, 2003.
72. *Liposome Technology*; Gregoriadis, G., Ed.; Informa Healthcare: London, 2006. 3rd ed.
73. Deissler, V.; Rüger, R.; Frank, W.; Fahr, A.; Kaiser, W. A.; Hilger, I. *Small* **2008**, *4*, 1240.
74. Jeong, H.-S.; Lee, C.-M.; Cheong, S.-J.; Kim, E.-M.; Hwang, H.; Na, K. S.; Lim, S. T.; Sohn, M.-H.; Jeong, H.-J. *J. Liposome Res.* **2013**, *23*, 291.
75. Proulx, S. T.; Luciani, P.; Derzsi, S.; Rinderknecht, M.; Mumprecht, V.; Leroux, J.-C.; Detmar, M. *Cancer Res.* **2010**, *70*, 7053.
76. Al-Jamal, W. T.; Kostarelos, K. *Acc. Chem. Res.* **2011**, *44*, 1094.
77. Suganami, A.; Toyota, T.; Okazaki, S.; Saito, K.; Miyamoto, K.; Akutsu, Y.; Kawahira, H.; Aoki, A.; Muraki, Y.; Madono, T.; Hayashi, H.; Matsubara, H.; Omatsu, T.; Shirasawa, H.; Tamura, Y. *Bioorg. Med. Chem. Lett.* **2012**, *22*, 7481.
78. Rice, B. W.; Cable, M. D.; Nelson, M. B. *Biomed. Opt.* **2001**, *6*, 432.
79. Keshtgar, M. R. S.; Ell, P. J. *Eur. J. Nucl. Med.* **1999**, *26*, 57.
80. Tribet, C.; Vial, F. *Soft Matter* **2008**, *4*, 68.
81. Kashiwayanagi, M.; Suenaga, A.; Enomoto, S.; Kurihara, K. *Biophys. J.* **1990**, *58*, 887.
82. Lee, H. S.; Lee, H. E.; Park, D. J.; Park, Y. S.; Kim, H.-H. *Ann. Surg. Oncol.* **2012**, *19*, 772.
83. Ryu, K. W.; Eom, B. W.; Nam, B.-H.; Lee, J. H.; Kook, M. C.; Choi, I. J.; Kim, Y.-W. *J. Surg. Oncol.* **2011**, *104*, 578.
84. Jain, R.; Dandekar, P.; Patravale, V. *J. Controlled Release* **2009**, *138*, 90.
85. Melancon, M. P.; Zhou, M.; Li, C. *Acc. Chem. Res.* **2011**, *44*, 947.